Inorg. Chem. **2002**, *41*, 6274–6280

Syntheses, Structure, and Photoluminescence Properties of the 1-Dimensional Chain Compounds $[(TPA)_2Au][Au(CN)_2]$ and (TPA)AuCl (TPA = 1,3,5-Triaza-7-phosphaadamantane)

Zerihun Assefa,[†,‡] Mohammad A. Omary,[§,||] Brian G. McBurnett,[†,⊥] Ahmed A. Mohamed,[†] Howard H. Patterson,[§] Richard J. Staples,[#] and John P. Fackler, Jr.*[,†]

Department of Chemistry and Laboratory for Molecular Structure and Bonding, Texas A&M University, College Station, Texas 77843, Department of Chemistry, University of Maine, Orono, Maine 04469, and Department of Chemistry and Chemical Biology Harvard University, 12 Oxford Street, Cambridge, Massachusetts 02138

Received June 10, 2002

The structures and temperature-dependent photoluminescence properties of the one-dimensional compounds $[(TPA)_2Au][Au(CN)_2]$, **1**, and (TPA)AuCl, **2**, are reported. An extended linear chain with weak Au···Au interactions along the *c*-axis is evident in the structure of **1**, and a helical chain with a pitch of 3.271 Å is seen for **2**. The intrachain Au···Au separation is 3.457(1) and 3.396(2) Å in **1** and **2**, respectively. As a result of this weak Au···Au interaction, the physical properties of these compounds are anisotropic. Scanning electron microscopy (SEM) studies indicate that single crystals of both compounds are noninsulating. Single crystals of **1** do not luminesce visibly, but grinding the crystals finely initiates a strong green emission under UV irradiation at room temperature. Further interesting optical properties include the dependence of the emission profile of the powder on the exciting wavelength and luminescence thermochromism. When excited at wavelengths < 360 nm, the powder exhibits a blue emission at 425 nm while excitation with longer wavelengths leads to a green emission near 500 nm. While the green emission dominates at ambient temperature, cooling to cryogenic temperatures leads to the dominance of the blue emission. Fibers of **2** are luminescent at 78 K with an emission band centered at 580 nm. Compound **1** crystallizes in the orthorhombic space group *Cccm* (No. 66), with $Z = 2$, $a = 6.011(1)$ Å, $b = 23.877(6)$ Å, $c = 6.914(1)$ Å, $V = 992.3(3)$ Å^3, and $R = 0.0337$. Compound **2** crystallizes in the trigonal space group $R\bar{3}$ (No. 148), with $Z = 18$, $a = 22.587(2)$ Å, $b = 22.587(2)$ Å, $c = 9.814(2)$ Å, $V = 4336$ Å^3, and $R = 0.0283$.

Introduction

The physical properties of 1-dimensional chain or 2-dimensional sheet compounds are determined by the shape of the molecular units, their electronic structures, and overlap of metal orbitals between neighbors.[1] Planar molecules with no bulky ligand components allow close contact and a strong interaction between the molecules in a chain. Intrachain interactions between molecular units depend on the presence of electrons in orbitals with relatively large extensions perpendicular to the axis (linear molecule) or plane of the molecule.[1] The tetracyanoplatinates(II) represent a class of widely investigated compounds in this regard that show columnar structures in the solid state.[2] The two-dimensional $MAu(CN)_2$ and $MAg(CN)_2$ complexes also have been studied extensively and show interesting photoluminescence, PL, properties that have been correlated with Au···Au and Ag···Ag interactions.[3,4] Schmidbaur and co-workers showed that the aurophilic aggregation, which leads to dimers and

* To whom correspondence should be addressed. E-mail: fackler@mail.chem.tamu.edu.
[†] Texas A&M University.
[‡] Permanent address: Chemical Sciences Division, Oak Ridge National Laboratory, Oak Ridge, TN 37831-6375.
[§] University of Maine.
[||] Permanent address: Department of Chemistry, University of North Texas, P.O. Box 305070, Denton, TX 76203.
[⊥] Permanent address: Department of Chemistry, California State University, Chico, CA, 95929-0210.
[#] Harvard University.

(1) Nigrey, P, J. In *Extended Linear Chain Compounds*; Miller, J. S., Ed.; Plenum Press: New York, 1983.
(2) (a) Ammon, W. V.; Hidvegi, I.; Gliemann, G. *J. Chem. Phys.* **1984**, *80*, 2837. (b) Gliemann, G.; Yersin, H. *Struct. Bonding* **1985**, *62*, 89. (c) Yersin, H. *J. Chem. Phys.* **1982**, *77*, 2266.

10.1021/ic025784r CCC: $22.00
Published on Web 10/31/2002

extended polymeric arrays for gold(I) complexes, can be controlled by ligand steric factors which dominate over the weak (5−10 kcal/mol) Au···Au bonding.[5]

In this paper wherein the sterically undemanding TPA[6] ligand is used, it is shown that the state of aurophilic aggregation observed also depends on thermodynamic crystallization factors such as solvent incorporation, ionic lattice forces, and H-bonding of the ligand. Eisenberg and coworkers[7] recently utilized the crystallization behavior of some luminescent Au(I) dithiocarbamates to develop a sensor for volatile organic compounds (VOC's), results similar to those of Mann[8] using linear chain [M(NCR)$_4$][M(CN)$_4$], M= Pd and Pt, complexes. The "(TPA)AuCN" species described here contains a linear chain of alternating cations and anions, [(TPA)$_2$Au][Au(CN)$_2$], **1**. However, its analogue, Me$_3$-PAuCN, is structurally similar[9] to the species (TPA)AuCl, **2**, which contains no lattice solvent molecules. This latter compound is structurally different[6a] from solvent-containing (TPA)AuCl·CH$_3$CN and the protonated, H-bonded species (TPA−HCl)AuCl·0.5H$_2$O, both of which are crossed molecular dimers. The interesting PL properties of **1** and **2** are described here.

Experimental Section

Synthesis. Complex **1**, bis(1,3,5-triaza-7-phosphaadamantane)-gold(I) dicyanoaurate(I), [(TPA)$_2$Au][Au(CN)$_2$], was synthesized by slowly adding an aqueous solution of KAu(CN)$_2$ to a [(TPA)$_2$Au]-Cl solution in a 1:1 ratio. The mixture was left undisturbed for slow evaporation. Clear colorless crystals emerged after a few hours. The mother liquor was carefully removed, and the crystals were dried in air. The IR, ν(C−N), is observed at 2143 cm^{-1}. Compound **2**, (TPA)AuCl, was synthesized as reported earlier.[6a] By diffusion of *n*-hexane into a 1,2-dichloroethane solution, long fibers of **2** were obtained with no solvent in the lattice.

Structural Data. The structures of **1** and **2** were determined with data collected on a Nicolet R3m/E diffractometer (SHELXTL 5.1) by employing Mo Kα radiation (λ = 0.710 73 Å) using a procedure described earlier.[6a] The unit cell constants were determined from 25 machine-centered reflections. Empirical absorption corrections based on azimuthal (ψ) scans of reflections were applied for both structures. For **1**, disorder along the Au···Au axis puts the cation and anion at the same apparent position and requires the CN group and the TPA ligand to be modeled at 50% of their proper occupancy. The Au atom sits at the origin in the *Cccm* space group that was chosen, giving an apparent *I*-centered cell. The TPA ligand resides on the mirror plane, and the CN atoms are at general positions. Other space groups considered gave poorer statistics or unsatisfactory models. A colorless needle of **2** with dimensions of 0.4 × 0.08 × 0.08 mm^3 was mounted on a glass fiber with epoxy cement at room temperature. Data collected with the ω-scanning procedure and subsequent data refinement proceeded normally. The compound crystallizes in the trigonal system, and the space group is $R\bar{3}$ (No. 148) as confirmed by the successful refinement of the structure.

Table 1. Crystal Data for **1** and **2**

param	**1**	**2**
chem formula	$C_{14}H_{24}N_8P_2Au_2$	$C_6H_{12}N_3PAuCl$
fw	760.29	389.6
cryst syst	orthorhombic	trigonal
space group	*Cccm* (No. 66)	$R\bar{3}$ (No.148)
a, Å	6.011(1)	22.587(2)
b, Å	23.877(6)	
c, Å	6.914(1)	9.814(2)
V, Å^3	992.3(3)	4336(1)
Z	2	18
μ, mm^{-1}	14.945	15.638
D_{calcd}, g cm^{-3}	2.544	2.686
T, K	293	298
λ, Å	0.710 73	0.710 73
R1[a] [$I > 2\sigma(I)$]	0.0337	0.0283
wR2[b] [$I > 2\sigma(I)$]	0.0791	0.0274

[a] $R1 = \sum||F_o| - |F_c||/\sum|F_o|$. [b] $wR2 = \{\sum[w(F_o^2 - F_c^2)^2]/\sum[w(F_o^2)^2]\}$.

Spectroscopy. Emission spectra at 77 K and ambient temperature were recorded as previously described[6] with a model 8100 SLM AMINCO spectrofluorometer using a 150 W Xe lamp excitation. Temperature-dependent steady-state and lifetime measurements were conducted at the University of Maine. Liquid helium was used as the coolant using a model LT-3-110 Heli-Tran cryogenic liquid transfer system. The steady-state spectra were recorded with a model QuantaMaster-1046 PTI spectrofluorometer, which is equipped with two excitation monochromators and a 75 W xenon lamp. Correction of the excitation spectra was carried out using the quantum counter rhodamine B. The lifetime data were acquired with a Molectron UV series 14 pulsed nitrogen laser using the procedure described elsewhere.[10] Scanning electron micrographs were obtained at the Texas A&M Electron Microscopy Center using a JEOL 6400 microscope on single crystals of **1** and **2** placed on a carbon tape without being coated with a conducting material.

Results

Structural. Crystallographic data for compounds **1** and **2** are recorded in Table 1. Selected bond lengths and angles for **1** and **2** are listed in Table 2. Figure 1 presents a thermal ellipsoid drawing for the structure of [(TPA)$_2$Au][Au(CN)$_2$], **1** (TPA = 1,3,5-triaza-7-phosphaadamantane). The asymmetric unit contains one monovalent gold atom with the other

(3) (a) Patterson, H. H.; Roper, G.; Biscoe, J.; Ludi, A.; Blom, N. *J. Lumin.* **1984**, *31/32*, 555. (b) Markert, J. T.; Blom, N.; Roper, G.; Perregaux, A. D.; Nagasundaram, N.; Corson, M. R.; Ludi, A.; Nagle, J. K.; Patterson, H. H. *Chem. Phys. Lett.* **1985**, *118*, 258. (c) Assefa, Z.; DeStefano, F.; Garepapaghi, M.; LaCasce, J., Jr.; Ouellete, S.; Corson, M.; Nagle, J.; Patterson, H. H. *Inorg. Chem.* **1991**, *30*, 2868. (d) Nagle, J.; LaCasce, J., Jr.; Corson, M.; Dolan, P. J., Jr.; Assefa, Z.; Patterson, H. H. *Mol. Cryst. Liq. Cryst.* **1990**, *181*, 356. (e) Assefa, Z.; Shankle, G.; Reynolds, R.; Patterson, H. H. *Inorg. Chem.* **1994**, *33*, 2187.

(4) (a) Omary, M. A.; Patterson, H. H. *J. Am. Chem. Soc.* **1998**, *120*, 7696. (b) Rawashdeh, M. A.-O.; Omary, M. A.; Patterson, H. H.; Fackler, J. P., Jr. *J. Am. Chem. Soc.* **2001**, *123*, 11237 and references therein.

(5) Angermaier, K.; Zeller, E.; Schmidbaur, H. *J. Organomet. Chem.* **1994**, *472* (1−2), 371.

(6) (a) Assefa, Z.; McBurnett, B. G.; Staples, R. J.; Fackler, J. P., Jr.; Assman, B.; Angermaier, K.; Schmidbaur, H. *Inorg. Chem.* **1995**, *34*, 75. (b) Assefa, Z.; McBurnett, B. G.; Staples, R. J.; Fackler, J. P., Jr. *Inorg. Chem.* **1995**, *34*, 4965. (c) Forward, J. M.; Fackler, J. P., Jr.; Assefa, Z. In *Optoelectronic Properties of Inorganic Compounds*; Roundhill, D. M., Fackler, J. P., Jr., Eds.; Plenum Press: New York, 1999; pp 195−229.

(7) Mansour, M. A.; Connick, W. B.; Lachicotte, R. J.; Gysling, H. J.; Eisenberg, R. *J. Am. Chem. Soc.* **1998**, *120*, 1329.

(8) (a) Daws, C. A.; Exstrom, C. L.; Sowa, J. R. J.; Mann, K. R. *Chem. Mater.* **1997**, *9*, 363. (b) Exstrom, C. L.; Pomije, M. K.; Mann, K. R. *Chem. Mater.* **1998**, *10*, 942.

(9) Ahrland, S.; Aurivillius, B.; Dreisch, K.; Noren, B.; Oskarsson, A. *Acta Chem. Scand.* **1992**, *46*, 262.

(10) Nagasundaram, N.; Roper, G.; Biscoe, J.; Chai, J. W.; Patterson, H. H.; Blom, N.; Ludi, A. *Inorg. Chem.* **1986**, *25*, 258.

Table 2. Selected Bond Distances (Å) and Angles (deg) for Compounds **1** and **2**

	1		2	
	dists, Å	angles, deg	dists, Å	angles, deg
Au(1)−Au(1a)	3.457(1)		3.394 (1)	
Au(1)−P(1)	2.302(5)		2.224	
Au(1)−P(1a)	2.302(5)			
Au(1a)−C(5)	2.02(3)			
Au(1)−C(5b)	2.02(3)			
Au−Cl			2.299(4)	
P(1)−Au(1)−P(1a)		180		
C(5)−Au(1)−C(5b)		179.998(2)		
P−Au−Cl				177.6
Newman projection		27.0		63.3

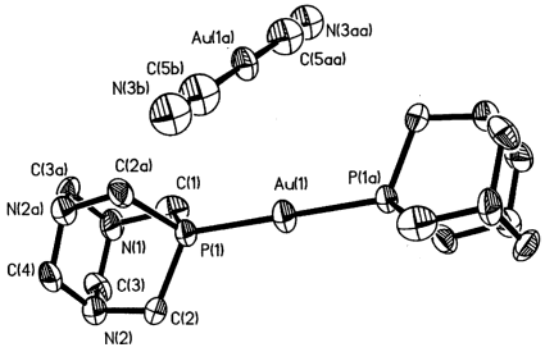

Figure 1. Thermal ellipsoid drawing of **1** at 50% probability.

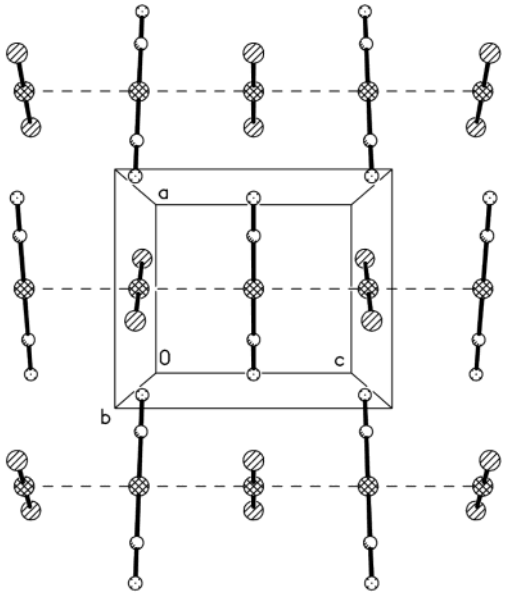

Figure 2. Packing diagram showing the linear chain structure of **1**. For clarity, only phosphorus atoms in the TPA ligand are shown.

gold atom generated by symmetry. The compound crystallizes in the orthorhombic space group *Cccm* (No. 66). The Au(1) is coordinated linearly to the two TPA ligands while Au(1a) is coordinated linearly to the two CN^- ligands (Figure 1). The anion portion of the molecule C−Au−C is rotated away from the P−Au−P axis of the cation by an angle of 27°. The Au−P distances, 2.302(5) Å, are identical by symmetry. The Au(1) and Au(1a) centers alternate along the *c*-axis, forming an infinite one-dimensional (1-D) linear chain (Figure 2). The Au···Au separation of 3.457 Å between the cation and anion centers is uniform along this axis.

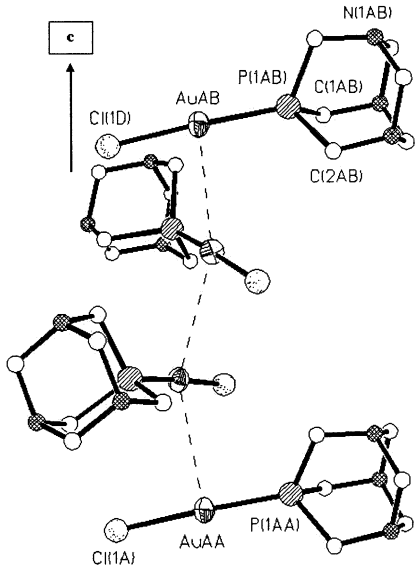

Figure 3. Thermal ellipsoid drawing of a full helix of **2** along the *c*-axis at 50% probability.

Figure 3 presents a thermal ellipsoid drawing for the structure of (TPA)AuCl, **2** (TPA = 1,3,5-triaza-7-phosphaadamantane). Compound **2** crystallizes in the trigonal space group $R\bar{3}$. A CH_3CN-solvated structure for this compound has been reported[6a] wherein (TPA)AuCl units dimerize, producing a short Au···Au contact of 3.09 Å. In contrast, the unsolvated compound **2** polymerizes with an infinite helical chain of gold atoms and a much longer but uniform separation of 3.396(2) Å between the Au(I) atoms (Figure 3). While the geometry around each gold atom is nearly linear, the angle between the crossed "lolly pop" (aurophilically bonded) units in **2** is close to 60°, significantly smaller than the angle found[6a] in the solvated two unit species, 90°, but larger than this angle in **1** (27°). The P−Au−Au−P torsion angle in **2** is −116.8° with a Newman projection of 63.3° between units. The helix in **2** has a pitch of 3.271 Å.

Spectroscopic Studies. Since compounds **1** and **2** are one-dimensional systems, it was thought that some of their physical properties might show anisotropy along the chain axis. Scanning electron micrograph studies (SEM) were conducted to assess the conductivity of the uncoated single crystals of **1** and **2**. Shown in Figure 4a is the micrograph of single crystals of **1** taken without applying a conducting coating. The micrograph demonstrates that **1** is either a conductor or a semiconductor along the chain axis.[11] Similarly, **2** also shows a weak conducting behavior as evaluated from the SEM data shown in Figure 4b. Although spectroscopic attempts to estimate the band gap have not been successful, distinctly metallic properties are not anticipated in solids formed from these molecules. The IR spectrum of **1** shows a strong ν(C−N) symmetric stretch at 2143 cm^{-1}. This value is very similar to the 2141 cm^{-1} reported[12] for $KAu(CN)_2$. Electron density depletion from

(11) *Scanning Electron Microscopy and X-ray Microanalysis*; Goldstein, J. I., et al., Eds.; Plenum Press: New York, 1992.
(12) Stammreich, H.; Chadwick, B.; Frankiss, S. *J. Mol. Struct.* **1967**−**68**, *1*, 191.

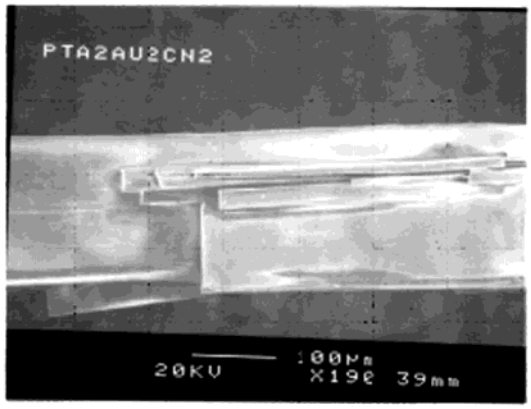

(a)

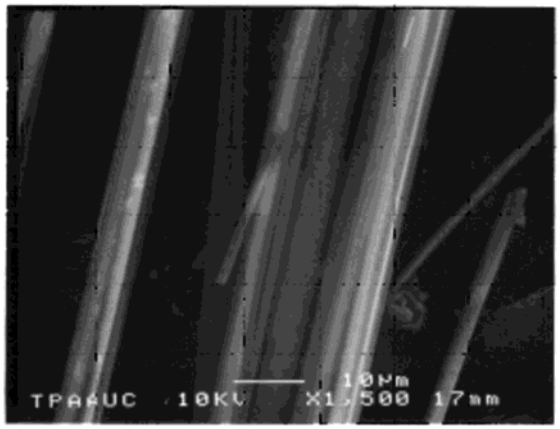

(b)

Figure 4. (a) Scanning electron micrograph of single crystals of **1**. The image observed indicates that crystals of **1** are conducting or semiconducting. The study was performed on a JEOL 6400 SEM instrument by attaching the single crystals to a carbon tape without the normal coating of the crystals with a conducting metal deposit. (b) Scanning electron micrograph of single crystals of **2** under the same conditions.

the metal centers is not evident from the CN vibrational frequency in these systems, presumably because intermolecular Au···Au interactions exist in both **1** and pure KAu(CN)$_2$.

A characteristic feature of **1** is that the compound does not appear to be luminescent in the visible region in the single crystal form but luminesces strongly when ground to a fine powder. The powder emission spectra of **1** are shown in Figure 5. Several factors affect the relative intensities of the blue and green emission bands displayed by the compound, including temperature and excitation wavelength.

At 78 K for **1**, the higher-energy (HE) blue emission band (λ_{max} = 425 nm) is dominant when the sample is excited at wavelengths < 365 nm (Figure 5a,b). However, when the excitation is changed to wavelengths longer than 365 nm, the intensity of the blue HE band drops sharply with a concomitant increase in the intensity of a broad lower-energy (LE) green emission band near 500 nm. As shown in Figure 5c, changing the excitation wavelength to 380 nm provides a spectral profile where the LE band at 500 nm dominates. Each of the two emission bands provides its own characteristic excitation profile. In Figure 6 are shown the excitation spectra of **1** monitored at the HE and LE emission bands.

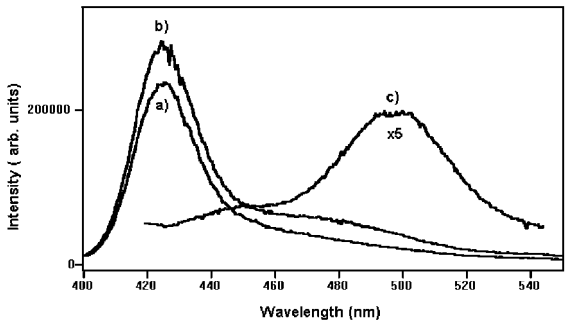

Figure 5. Dependence of the emission spectra of **1** on the excitation wavelength. The spectra were measured at 78 K and excited at (a) 320 nm, (b) 360 nm, and (c) 380 nm.

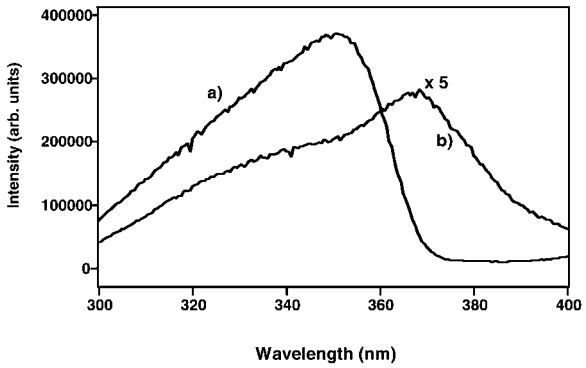

Figure 6. Excitation spectra of **1** monitored at the (a) 430 nm emission band and (b) 490 nm emission band.

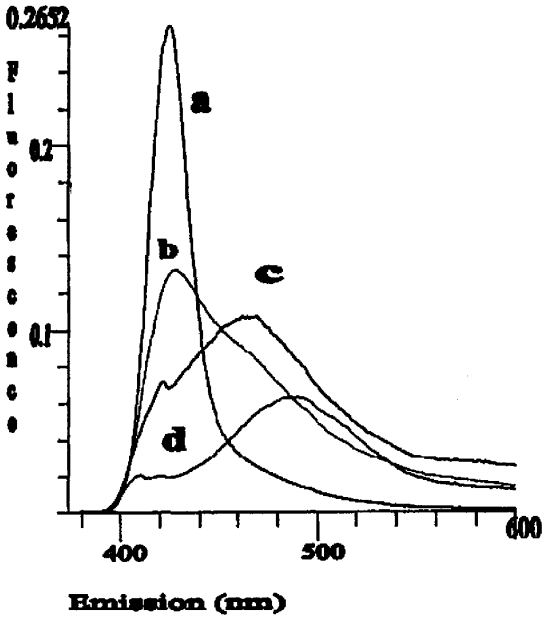

Figure 7. Temperature-dependent emission spectra of **1**: (a) 78 K; (b) 130 K; (c) 150 K; (d) 200 K.

The HE band corresponds to an excitation peak with a maximum at ca. 350 nm (Figure 6a), while the LE band corresponds to an excitation maximum at ca. 365 nm. The change from a blue to green emission is evident even visually when the excitation is changed to the longer wavelengths.

The temperature-dependent emission spectra of **1** are shown in Figure 7 under 350 nm excitation in the 78−298 K temperature range. Luminescence thermochromism be-

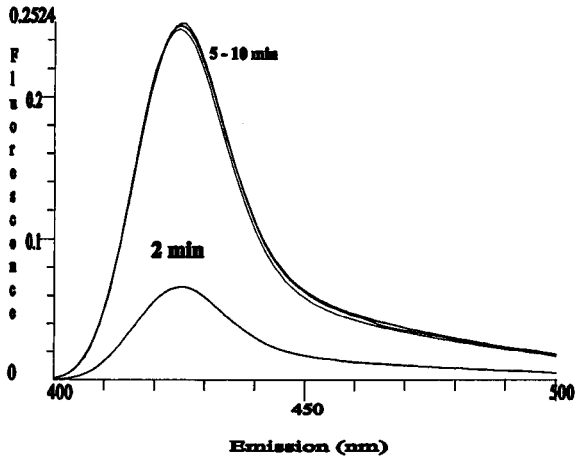

Figure 8. Relative emission intensity of compound **1** with respect to grinding time. The spectra were recorded at 78 K with an identical PMT gain, slit width, and other instrumental setup. No emission is evident before grinding the crystalline sample. Using acetone and MeOH as dispersant quenched the low-energy green emission, and only the blue emission band (maximum at 424 nm) was evident.

Table 3. Low-Temperature Lifetime Data for **1**

temp, K	emission band, nm	τ, ns
40	420	200, 1000
	490	<10
78	420	90, 540

tween the blue and green emission colors is evident both visually and spectrally; Figure 7 illustrates that the intensity of the blue emission decreases with increasing temperature. As a result, the green emission dominates at room temperature while spectra acquired at 20 K (not shown) show the dominance of the blue emission over the green emission by about 23 times. Visual inspection indicates that under UV excitation the intensity of the green visible emission of powdered **1** at room temperature increases with increased grinding of the sample. We have attempted to correlate the emission intensity with the grain size of the powder.[13] In Figure 8, the emission intensity is shown as a function of grinding time. No dispersant has been used in this measurement. With 0−4 min of grinding the emission intensity increases but stays constant with longer grinding times.

Lifetime data corresponding to 40 and 78 K are given in Table 3. The high-energy emission, which was measured at 420 nm, shows a biexponential decay with lifetimes of 0.20 and 1.0 μs. When the data are recorded at 78 K, both lifetimes become shorter and provide values of 0.092 and 0.54 μs, respectively. On the other hand the LE band which was measured at 490 nm shows a very short lifetime of <10 ns even at 40 K. Due to instrumental limitations we were unable to measure the lifetime of this LE band accurately.

(13) Unfortunately, particle size measurements (using scanning electron microscopy) have not been successful due to the lack of a good dispersant. In addition, grinding in acetone and MeOH results in particle aggregation, preventing particle size determination. Samples that were ground in acetone and MeOH as dispersants show quenching of the LE green emission, with only the HE emission observed. A similar quenching of the green emission has not been observed upon grinding the sample under glycerol and/or other higher molecular weight alcohols.

Discussion

Structural Studies. Few other mononuclear gold(I) complexes have been characterized to date which show a linear chain arrangement similar to that found in compounds **1** and **2**. For example, in the chain pyridine solvates of gold(I) halides, "pyAuCl", the gold atom is present alternately as a solvato complex $[Au(py)_2]^+$ and as a dihalo complex, $[AuCl_2]^-$ forming the linear chain.[14] In the structure of $[(tht)_2Au][AuI_2]$ (tht = tetrahydrothiophene) the gold atoms are arranged in a zigzag chain with relatively short Au−Au distances of 2.967 and 2.980 Å.[15] Schmidbaur and co-workers have reported a variety of haloisonitrilegold(I) compounds showing polymeric chain or sheet structures as well as dimers.[16] An infinite chain of gold atoms also has been found in $\{[AuS_2P(O\text{-}i\text{-}C_3H_7)_2]_2]\}_n$, where dinuclear units with a short metal−metal separation of 2.914 Å polymerize.[17] A similar structure has been observed with $[AuCH_2P(S)Ph_2]_2$.[18] Compounds containing linear chains of heterobimetallic units, Au−Tl and Au−Pb−Au, with short metal−metal separations also have been reported.[19] The Au···Au separations observed in **1** and **2** are relatively long when compared to some of these compounds, however. The separation more closely resembles that of the two-dimensional $MAu(CN)_2$ (M = K, Cs or Na) compounds,[3] where the intralayer Au···Au separation is significantly longer,[20] ranging from 3.2 to 3.6 Å.

Even though it has been shown that aurophilic aggregation, which leads to dimers and extended polymeric arrays for gold(I) complexes, is controlled by ligand steric factors, the structural features displayed by compounds **1** and **2** (with the sterically undemanding[6] TPA ligand) suggest that thermodynamic crystallization factors such as solvent incorporation, ionic lattice forces, and H-bonding of the ligand also can control the interaction. Thus, "(TPA)AuCN" described here contains a linear chain of alternating cations and anions so that the molecular formula of **1** is better represented as $[(TPA)_2Au][Au(CN)_2]$. Its analogue,[9] Me_3-PAuCN, is structurally like the species (TPA)AuCl, **2**, which contains no lattice solvent molecules. However, this latter compound is structurally different[6a] from (TPA)AuCl·CH_3-CN and the protonated/H-bonded species (TPA−HCl)-AuCl·$0.5H_2O$, both of which are crossed molecular dimers. An interesting observation that we noted in the structures of these complexes is that a correlation appears to exist between the angles of the aurophilically bonded units and the Au···Au distance. For example, in the solvated dimeric species of (TPA)AuCl·CH_3CN, where the angle between the P−Au−

(14) Adams, H.-N.; Hiller, W.; Strähle, J. *Z. Anorg. Allg. Chem.* **1969**, *23*, 3534.
(15) Ahrland, S.; Noren, B.; Oskarsson, A. *Inorg. Chem.* **1985**, *24*, 1330.
(16) Schneider, W.; Angermaier, K.; Sladek, A.; Schmidbaur, H. Z. *Naturforsch., B* **1996**, *51*, 790.
(17) Lawton, S. L.; Rohrbough, W. J.; Kokotailo, G. T. *Inorg. Chem.* **1972**, *11*, 2227.
(18) Mazany, A. J.; Fackler, J. P., Jr. *J. Am. Chem. Soc*. **1988**, *110*, 3308.
(19) Wang, S.; Garzòn, G.; King, C.; Wang, J.-C.; Fackler, J. P., Jr. *Inorg. Chem*. **1989**, *28*, 4623.
(20) (a) Baenziger, N. C.; Bennett, W. E.; Soboroff, D. M. *Acta Crystallogr*. **1976**, *B32*, 962. (b) Khan, M.; Oldham, C.; Tuck, D. G. *Can. J. Chem*. **1981**, *59*, 2714.

Au′ and Au−Au′−P planes is 90°, the Au···Au distance is shorter by 0.37 Å than in **2** (Newman projection angle of 63.3°). Similarly, the Au···Au distance is shorter by 0.06 Å in **2** than in **1**, where the projection angle is only 27°. Contrary to expectation, the cation−anion type electrostatic attraction in **1** has not resulted in any shortening of the Au···Au distance when compared to the neutral dimeric interactions found in **2** and its solvated analogues. Even in the case of (TPA−HCl)AuCl·0.5H_2O, where two formally cationic centers interact, the Au···Au distance is shorter than that found in **1**. Our data suggest that expansion in the Au···Au distance is accompanied by a decreased projection angle which, in turn, leads to the observation of a polymeric structure rather than the dimer. While our current understanding of these linear chain structures is very limited, with no cause nor effect implied, these observations may help develop a rational design and synthesis of inorganic polymeric materials involving aurophilic Au···Au interactions.

Luminescence Studies. The importance of Au···Au interactions in influencing the PL properties of Au(I) complexes is now well recognized.[6c,21] Many compounds containing a polymeric structure of gold atoms are known to luminesce at relatively low energy,[3] and their optical properties are dictated by anisotropic effects.[2,18] Similarly, the Au···Au interactions are important in understanding the photoluminescence behavior exhibited by **1**. One of the starting materials in the synthesis of **1**, (TPA)$_2$AuCl, is not luminescent and shows no Au···Au interaction in its crystal structure.[22] The other starting compound, KAu(CN)$_2$, is luminescent but at a significantly higher energy, $\lambda_{em} = 390$ nm.[3] The gold atoms in KAu(CN)$_2$ are arranged in 2-D sheets[18] with an Au···Au separation of 3.6 Å, which is longer than that found in **1**.

The optical properties of **1** are especially striking in that the compound is not visibly luminescent as a single crystal but luminesces strongly as a powder. Large single crystals of **1** are not visibly luminescent even at cryogenic temperatures, and the green luminescence appears only after grinding the solid finely. This behavior was initially thought to arise as a consequence of a phase change that may accompany grinding. However, the X-ray powder pattern of the finely ground material remained indexed as calculated from the single-crystal data. Thus, a phase transformation has been ruled out as the origin for the luminescence behavior exhibited. Although, the long-range ordering in **1** has not been affected as a result of grinding, it should be noted that effects on short-range ordering may not be noticeable by the X-ray data. After considering other mechanisms, we believe that the luminescence in **1** can be attributed to changes that may occur near the surface of the material and/or formation of defect sites.

The periodicity of a perfect lattice breaks down at a surface. Single crystals contain relatively few chain terminations at the surface compared with a finely ground powder. Surfaces and mosaic spread cause interruptions in the periodic nature of the linear chains and can give rise to trapping levels in the periodic electronic potential within the forbidden gap in the surface region. Usually, such trapping levels are shallow and thus the energy required to free the electron or hole from the trap is small.[23] Grinding not only increases the surface area, thus exposing more chain ends, it also increases mosaic spread and creates lattice defects. Although the exact nature of the defect centers has not been understood fully, it is clear that grinding induces mechanical stress and bonding rearrangement at the site of chain termination. Our studies of **1** suggest that the emission from the powder originates from several localized defect sites which show little communication with each other. This is supported by the above finding that two emission bands at 425 and 500 nm were obtained, each with a characteristic excitation profile. In fact, when the luminescence detection is enhanced by carrying out experiments with liquid helium as the coolant, the presence of more such trapped sites became apparent. For example, Figure 9 shows that at least four emission bands with peaks near 425, 450, 485, and 545 nm were obtained for a powdered crystal of **1** at 20 K by varying the excitation wavelength.

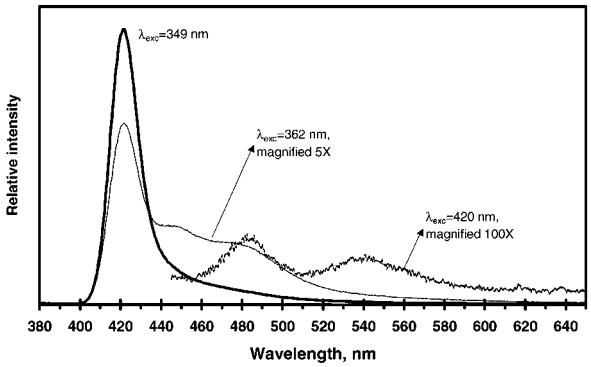

Figure 9. Emission spectra of a powdered crystal of **1** at 20 K using different excitation wavelengths as shown.

The 425 emission band shows a biexponential decay, suggesting that the emission originates from two closely spaced states. Compared to the HE band, the emission at 490 nm has a much shorter lifetime (<10 ns) and shows no temperature influenced quenching. A mechanism where the LE level is populated via cascading of the excitation from the higher level is inconsistent with the lifetime result since lack of communication between the emitting levels is evident from the data. Observance of two different excitation profiles for the two emission bands also supports this conclusion. In addition, the fact that the high-energy emission is quenched at room-temperature corroborates the argument that the emission originates from a shallow trap. Thus, it is suggested that the observed visible emission in this system originates from lattice defect centers that operate independently and with little communication between them. Since the chains in **1** run parallel to the long crystal axis, grinding exposes more chain ends. It is reasonable to expect that the Au···Au distances at the chain ends are shorter than in the bulk; thus,

(21) Fackler, J. P.; Grant, T. A. *Chemist* **1998**, *75*, 29.
(22) Assefa, Z.; Staples, R. J.; Fackler, J. P., Jr. *Acta Crystallogr.* **1996**, *C52*, 305.
(23) *Thermoluminescence of Solids*; McKeever, S. W. S., Ed.; Cambridge University Press: New York, 1985.

the emission becomes more like the emission observed with discrete dimers, a lower-energy emission dependent on the metal−metal distance.

Without grinding the single crystals, the metal-based emission associated with the surface molecules at the fiber ends is apparently too weak to be observed. This observation is to be contrasted with the observations of Eisenberg wherein disruption of the linear chains of Au(I) dithiocarbamates quenches the luminescence. However, unlike the luminescent dimeric (TPA)AuX·CH_3CN (X = Cl, Br) complexes, the S−Au−S units in the discrete dinuclear dithiocarbamates and related dithiophosphinates[24] are nearly coparallel (the twist generally is much less than 40°). While these nonlinear chain molecules visibly luminesce (LMCT) at low temperature, the luminescence generally is quenched at room temperature.[25]

Numerous examples of optical consequences of grinding have been noted previously, which range from induction of triboluminescence to emission quenching. In zirconia-based materials, for example, quenching of emission from finely ground samples has been noted and associated with enhancement of defect centers.[26] Initiation of UV-excited luminescence through grinding of single crystals has been documented previously in few cases but without thorough investigation of the origin of the phenomenon. It was reported previously[27] that crystals of Ph_3PAuCl luminesce after grinding the solid finely. In a study involving $KAu(CN)_2$, grinding of the single crystals has been found to alter the emission behavior.[10] A new emission band, assigned to surface states, has been reported to emerge at ca. 430 nm.[3,10] Another related study is that of Harvey and co-workers,[28] who attributed the low-energy visible emissions of diisocyano polymers of Ag(I) and Cu(I) to energy transfer delocalized along the metal−metal chains that terminate at the surface. In another study, Balch and co-workers reported solvent-stimulated phosphorescence in stacked trinuclear Au(I) complexes that had been exposed to UV irradiation.[29] The resulting orange phosphorescence was attributed to the storage of energy along the metal stacks during irradiation and its release at the surface sites, which are exposed by contact with solvent. The disruption of the chain structure caused by solvent contact is not dissimilar to the disruption of the chain structure of **1** caused by grinding the crystals.

Single crystals of **2** emit very weakly at 78 K, $\lambda_{max} = 580$ nm. The CH_3CN solvated species exists as a discrete crossed "lollipop" dimers which shows a strong, low-energy, $\lambda = 674$ nm, emission at 78 K. As pointed out previously,[6] the emission energy can be sensitive to the Au···Au distance. This behavior has been associated with a metal-centered excitation and emission process in which the HOMO−LUMO gap shrinks proportionately to the Au···Au distance. The results obtained for **2**, although incomplete, further confirm the previous assignments made for the protonated and unprotonated (TPA)AuC1 complexes.[6] However, an attempt to make a quantitative correlation of the emission energy with the Au···Au distance as found for the dimers underestimates by 0.14 Å the observed, 3.39 Å, Au···Au separation in this linear chain system. While polymerization clearly destabilizes the HOMO as does dimer formation, a quantitative correlation of the emission energy with the Au···Au distance observed in the polymer cannot be made without also knowing the density of states along the chain.

Conclusions

The two compounds studied in this work display an extended linear and a helical chain in their structures that consist of weak Au···Au interactions. The intrachain Au···Au separation is 3.457(1) and 3.396(2) Å in **1** and **2**, respectively. As a result of this weak Au···Au interaction, some of the physical properties of these compounds are anisotropic. Scanning electron microscopy (SEM) studies confirm that single crystals of both compounds are conducting or semiconducting. Single crystals of **1** do not luminesce, but grinding the crystals finely initiates a strong green emission under UV irradiation at room temperature. The emission band of the powder at 78 K centers at 425 nm when excited at <365 nm. When the sample is excited at a longer wavelength, the intensity of the high-energy emission band decreases drastically and the band at 500 nm dominates. Lifetime measurements verified that there exist little communication between the various emitting levels. It is thought that localized surface defects comprising dimeric or oligomeric units are responsible for the emission in the powder.

Acknowledgment. We thank the National Science Foundation, Grant CHE-9300107, the Robert A. Welch Foundation, the Texas Advanced Research Program, and the donors of the Petroleum Research Fund, administered by the American Chemical Society, for the support of this research. We thank Professor Joel S. Miller (U. Utah) for repeating the grinding and luminescence measurements of **1** and measuring the X-ray powder pattern of the material. The synthesis of a sample of **1** used for lifetime measurement by Tiffany Grant is kindly acknowledged.

Supporting Information Available: Tables listing detailed crystallographic data, atomic positions, parameters, and bond lengths and angles for compounds **1** and **2**. This material is available free of charge via the Internet at http://pubs.acs.org.

IC025784R

(24) van Zyl, W. E.; Staples, R. J.; Fackler, J. P., Jr. *Inorg. Chem. Commun.* **1998**, *1*, 51.
(25) Forward, J. M.; Bohmann, D.; Fackler, J. P., Jr.; Staples, R. J. *Inorg. Chem.* **1995**, *34*, 6330.
(26) Paje, S. E.; Lopis, J. L. *J. Phys. Chem. Solids* **1994**, *55*, 671.
(27) (a) Rosenzweig, A.; Cromer, D. *Acta Crystallogr.* **1959**, *12*, 709. (b) Blom, N.; Ludi, A.; Burgi, H.-B.; Tichy, K. *Acta Crystallogr.* **1984**, *C40*, 1767.
(28) Fortin, D.; Drouin, M.; Turcotte, M.; Harvey, P. D. *J. Am. Chem. Soc.* **1997**, *119*, 531.
(29) Vickery, J. C.; Olmstead, M. M.; Fung, E. Y.; Balch, A. L. *Angew. Chem., Int. Ed. Engl.* **1997**, *36*, 1179.